Development of a novel reagentless, screen–printed amperometric biosensor based on glutamate dehydrogenase and NAD^+, integrated with multi–walled carbon nanotubes for the determination of glutamate in food and clinical applications.

G. Hughes[1], R.M. Pemberton[1], P.R. Fielden[2], J.P. Hart[1*]

1. Centre for Research in Biosciences, Faculty of Health and Applied Sciences, University of the West of England, Bristol, Coldharbour Lane, Bristol, BS16 1QY

2. Department of Chemistry, Lancaster University, Bailrigg, Lancaster, United Kingdom, LA1 4YB

*Corresponding author: john.hart@uwe.ac.uk Tel: 0117 328 2469

Abstract

A screen printed carbon electrode (SPCE) containing the electrocatalyst Meldola's Blue (MB) has been investigated as the base transducer for a reagentless glutamate biosensor. The biopolymer chitosan (CHIT) and multiwalled carbon nanotubes (MWCNTs) were used to encapsulate the enzyme glutamate dehydrogenase (GLDH) and the co–factor nicotinamide adenine dinucleotide (NAD^+).

The biosensor was fabricated by sequentially depositing the components on the surface of the transducer (MB–SPCE) in a layer-by-layer process, details of which are included in the paper. Each layer was optimized to construct the reagentless device.

The biosensor was used in conjunction with amperometry in stirred solution using an applied potential of +0.1V (vs. Ag/AgCl). Optimum conditions for the analysis of glutamate were found to be: temperature, 35°C; phosphate buffer, pH 7 (0.75 mM, containing 0.05 M NaCl).

The linear range of the reagentless biosensor was found to be 7.5 μM to 105 μM, and limit of detection was found to be 3 μM (based on n = 5, CV: 8.5% based on three times signal to noise) and the sensitivity was 0.39 nA/μM (± 0.025, coefficient of variation (CV) of 6.37%, n = 5). The response time of the biosensor was 20 – 30 seconds.

A food sample was analysed for monosodium glutamate (MSG). The endogenous content of MSG was 90.56 mg/g with a CV of 7.52%.

The reagentless biosensor was also used to measure glutamate in serum. The endogenous concentration of glutamate was found to be 1.44 mM (n = 5), CV: 8.54%. The recovery of glutamate in fortified serum was 104% (n = 5), CV of 2.91%.

Keywords: Amperometric glutamate biosensor, Screen-printed, Multiwalled Carbon Nanotubes (MWCNTs), Reagentless.

1. Introduction

Glutamate is the principal excitatory neurotransmitter and a precursor for GABA, the primary inhibitory neurotransmitter. Deficiencies in the behaviour of neurological pathways that utilize glutamate and its receptors are associated with autism [1], stroke [2], Alzheimer's disease [3], schizophrenia [4] and depression [5]. Glutamate is also a vital compound in cellular metabolism as it is associated with transamination, a key step in amino acid degradation, and is formed during deamination. Consequently the measurement of glutamate in biological fluids is of considerable interest. In addition, the widespread use of monosodium glutamate (MSG) in food products has led to increased interest in the use of new measurement methods for glutamate levels in food [6].

In a previous paper we have reported on an approach to glutamate biosensor development, based on a screen–printed biosensor incorporating a redox mediator and glutamate dehydrogenase (GLDH). In that approach the required enzyme cofactor, nicotinamide adenine dinucleotide (NAD^+), was added into the analyte solution containing glutamate; the disposable biosensor was successfully applied to the analysis of serum and stock cubes [7]. While successful, the main drawback of this approach for a commercial biosensor is the requirement to add the cofactor into the sample solution.

Carbon nanotubes (CNTs) are renowned for their unique electronic and mechanical properties [8]. They possess a high active surface area, excellent biocompatibility [9] and the ability to facilitate redox reactions with fast electron–transfer rates [10]. These abilities have popularised CNTs in the development of electrochemical biosensors.

Two forms of CNT exist; single walled CNT (SWCNTs) and multi–walled CNT (MWCNTs). SWCNTs possess a singular graphite sheet rolled into a tube to create a cylindrical nanostructure, whereas MWCNT consist of several shells of cylindrical tubes.

Integration of redox dyes such as Meldola's Blue (MB) into MWCNT matrices, has been previously demonstrated with well–defined voltammetric responses [11]–[13]. It should be mentioned that the electrocatalyst MB greatly reduces the over-potential for the oxidation of NADH [14].

The low solubility of unmodified MWCNTs leads to poor homogenous dispersion, thus in the present study the MWCNTs were suspended in a solution containing chitosan (CHIT). CHIT is a natural polysaccharide derived from crustaceans, which enhances enzyme stability and possesses good film forming properties [15], [16]. The dispersion of CNTs was possible due to the low pH required to solubilise the CHIT (pH < 3.0) [17], which was achieved using HCl. It was reported that the dispersion of MWCNTs in CHIT/HCl compared with other solvents gave the smallest particle sizes and resulted in the formation of a greater surface area without the need for functionalization.

It has previously been reported that NAD^+ was readily integrated into a glucose dehydrogenase biosensor and did not leach from the MWCNT matrix when coated onto the surface of a glassy carbon electrode [18]. This was achieved utilising a layer-by-layer assembly procedure. Other researchers have reported on the layer-by-layer immobilisation method using modified CNTs to immobilise glutamate oxidase [19], [20] and horse radish peroxidase [21]. This procedure is regarded as a simple, inexpensive and highly versatile method for the incorporation of components into film structures [22]. The advantages of a reagentless device fabricated using this approach is that it leads to a low cost biosensor which is convenient to use as no additional cofactor is required to be added to the sample solution [23], [24].

This paper describes the steps involved in the layer-by-layer development of a fully reagentless amperometric biosensor for glutamate. The strategy employed to achieve this goal

has involved the integration of the biological components (enzyme and cofactor) with multi–walled carbon nanotubes (MWCNTs) on the surface of a Meldola's Blue screen–printed carbon electrode (MB–SPCE). The biosensor has been applied to the determination of glutamate in serum sample and stock cubes.

Based on the literature, it is believed that this is the first report on the development and application of a reagentless amperometric glutamate biosensor, based on GLDH and NAD^+ integrated with a disposable screen-printed electrode.

2. Materials and Methods

2.1. Chemicals and reagents

All chemicals were of analytical grade, purchased from Sigma Aldrich, UK, except glutamate dehydrogenase (CAT: 10197734001) which was purchased from Roche, UK. The 75 mM phosphate buffer (PB) was prepared by combining appropriate volumes of tri–sodium phosphate dodecahydrate, sodium dihydrogen orthophosphate dihydrate and disodium hydrogen orthophosphate anhydrous solutions to yield the desired pH. Glutamate and NADH/NAD^+ solutions were dissolved directly in 75 mM PB. Chitosan (CHIT) was dissolved in 0.05 M HCl (pH < 3.0) to produce a 0.05% solution following up to 10 minutes sonication. The multi-walled carbon nanotubes (MWCNT)/CHIT solution was prepared by mixing 0.6 mg of MWCNT into 300 µL solution of 0.05% of CHIT, with 15 minutes of sonication and stirring for 24 hours. Meldola's Blue (MB) in solution was prepared by dissolving the appropriate weight in distilled water. Fetal bovine serum (FBS) (South American Origin, CAT: S1810–500) obtained from Labtech Int. Ltd, was used for serum analysis. Food samples (Beef OXO cubes) were obtained from a local supermarket.

2.2. Apparatus

All electrochemical experiments were conducted with a three–electrode system consisting of a carbon working electrode containing MB, (MB–SPCE, Gwent Electronic Materials Ltd; Ink Code: C2030519P5), a Ag/AgCl reference electrode (GEM Product Code C61003P7); both printed onto PVC, and a separate Pt counter electrode. The area of the working electrode was defined using insulating tape, into a 3 x 3 mm square area. The electrodes were then connected to the potentiostat using gold clips. Solutions, when required, were stirred using a circular magnetic stirring disk and stirrer (IKA® C–MAG HS IKAMAG, Germany) at a uniform rate. A μAutolab II electrochemical analyser with general purpose electrochemical software GPES 4.9 was used to acquire data and experimentally control the voltage applied to the SPCE in the 10 ml electrochemical cell which was used for hydrodynamic voltammetry. An AMEL Model 466 polarographic analyser combined with a GOULD BS–271 chart recorder was used for all amperometric studies. Measurement and monitoring of the pH was conducted with a Fisherbrand Hydrus 400 pH meter (Orion Research Inc., USA). Sonications were performed with a Devon FS100 sonicator (Ultrasonics, Hove, Sussex, UK).

2.3. Principle of Operation of the Biosensor and Procedures

The overall principle of operation of the biosensor is shown in Fig 2. Glutamate in solution is oxidised to form 2–oxoglutarate in the presence of the immobilized enzyme glutamate dehydrogenase (GLDH) and NAD^+; the products NADH and NH_4^+ are formed during this

reaction. NADH chemically reduces Meldola's Blue which subsequently undergoes electrochemical oxidation at the electrode surface to produce the analytical response.

2.4. Procedures

2.4.1. Fabrication of the reagentless MWCNT–CHIT–MB/GLDH–NAD^+–CHIT/MWCNT–CHIT biosensor.

Fabrication was carried out using a layer-by-layer approach to produce a total of three layers. Solutions were drop-coated onto the $3mm^2$ carbon working electrode. Initial studies were performed to deduce the composition of layers 1 and 3. Figure 1 represents the layer-by-layer biosensor.

Layer 1 was formed by drop coating a 10µL mixture of MWCNTs suspended in a solution containing 0.05% CHIT in a 0.05M HCl solution. This layer was allowed to partially dry at 4°C under vacuum for 10 minutes.

Layer 2 was optimised by carrying out amperometric studies with biosensors constructed using different mass combinations of CHIT, NAD^+ with a fixed GLDH content of 27U (Table 1). This layer was allowed to dry at 4°C under vacuum for 3 hours.

Layer 3 was formed in the same manner as Layer 1. This layer was allowed to dry at 4°C under vacuum for 2 hours.

A further study into the effect of including additional MB was also performed. This was done by mixing in 1 µL of 0.01M MB in H_2O with the MWCNTs in layers 1 and 3. For layer 2, an additional 1 µL of 0.01M MB in H_2O was deposited at the composite surface. Biosensors were stored under a vacuum at 4°C when not in use. A photograph of the final biosensor is provided in the supplementary material (supplementary figure 5).

2.4.2. Hydrodynamic Voltammetry

Hydrodynamic voltammetry was performed using the complete biosensor with 400 µM of glutamate, in 0.75 mM phosphate buffer (pH 7.0) containing 50mM NaCl , in order to enzymatically generate NADH so as to establish the optimum operating potential for the amperometric determination of glutamate in food and serum samples. An initial potential of -120mV was applied to the biosensor and the resulting steady state current was measured; the potential was then changed to -115mV and again a steady state current was measured. The procedure was continued by changing the potential by 50mV steps to a potential of +100mV, with subsequent steps increasing by 25mV up to a final potential of +150mV. The steady state currents were measured at each potential, then a hydrodynamic voltammogram was constructed by plotting the steady state currents against the corresponding potentials.

2.4.3. Optimisation studies with the proposed biosensor using amperometry in stirred solution.

All amperometric measurements were performed with stirred 10mL solutions of 75mM PB pH 7.0 with 50mM NaCl (PBS), using an applied potential of +0.1 V vs. Ag/AgCl. In order to optimise the conditions the biosensor was immersed in a stirred buffer solution, the potential applied and sufficient time was allowed for a steady–state current to be obtained.

The optimisation of each component in layer 2 was performed by measuring the amperometric response to the additions of glutamate over the concentration range of 7.5 µM to 100 µM glutamate. The variations in the quantities of the components are shown in Table 1.

After the optimisation of the NAD^+ and CHIT components, the integration of additional 0.01M Meldola's Blue into each layer of the biosensor was investigated by amperometry.

Following optimisation of the individual biosensor components, studies into the effects of temperature and pH on the biosensor response were investigated. Optimum pH was determined by carrying out calibration studies over the pH range 5 – 9. A separate study was conducted to determine the optimum temperature. The temperature was varied over the range 25 – 40°C with the pH fixed at 7. The optimisation of the temperature and pH is displayed in the supplementary material (supplementary Fig 1 & Fig 2 respectively).

Table 1: This table displays combination of components found in layer 2.

GLDH (Units)	NAD^+ (µg)	CHIT (µg)
27	13.5	5
27	27	5
27	54	5
27	106	5
27	214	5
27	106	5
27	106	10
27	106	15
27	106	20

2.4.4. Application of optimised amperometric biosensor to the determination of glutamate in food.

An OXO cube was prepared by dissolving one cube in 50 mL of phosphate buffer and sonicating for 15 minutes. The endogenous concentration of MSG was determined by using the method of standard addition. An initial 5µl volume of the dissolved OXO cube was added

to the stirred buffered solution (10 mL) in the voltammetric cell containing the biosensor, operated at +0.1 V (vs. Ag/AgCl) with subsequent standard additions of 3 µL of 25 mM glutamate.

The reproducibility of the biosensor assay for MSG analysis in OXO cubes was determined by repeating the whole procedure five times with five individual biosensors.

2.4.5. Application of optimised amperometric biosensor to the determination of glutamate in serum.

The endogenous glutamate concentration of serum was determined by injecting an initial volume of 150 µL of serum into 9.85mL of buffer solution. Amperometry in stirred solution using an applied potential of +0.1V vs. (Ag/AgCl) was conducted with the serum solution. This was followed by additions of 3 µL aliquots of 25 mM standard glutamate solution to the voltammetric cell. The currents resulting from the enzymatic generation of NADH were used to construct standard addition plots, from which the endogenous concentration of glutamate was determined (n = 5). The reproducibility of the biosensor measurement was deduced by repeating the studies five times on a freshly diluted solution of the same serum with a fresh biosensor for each measurement.

The procedure was repeated using 50µL of serum spiked with 1.5 mM glutamate (n = 5) to determine to the recovery of the assay.

Due to the complex nature of the samples investigated, interferences such as ascorbic acid, sugars and other amino acids may be present. The possible effects of naturally occurring interferences from serum and OXO cubes were established using a dummy BSA biosensor. A dummy biosensor was constructed by drop coating the equivalent weight of the enzyme with BSA; however, no signals due to interfering substances were detected.

3. Results and Discussion

3.1. Characterisation of the biosensor using scanning electron microcroscopy (SEM) and amperometry

Figure 4 shows SEM images of the different layers deposited on top of the original Meldola's Blue SPCE (MB-SPCE). The only treatment of the biosensor specimens was a drying procedure.

Layer 1 (MWCNTs-CHIT-MB) is a porous open structure which shows the MWCNTs-CHIT deposited on the surface. The MB particles may be absorbed on both the exterior and interior of the MWCNTs.

Layer 2 appears to consist of a more cohesive film covering the added components (GLDH-NAD^+-CHIT-MB). The possibility of utilising this structure as a biosensor for glutamate was investigated, however, the amperograms did not display steady state currents. From this we deduced that the cofactor (NAD^+) and possibly the enzyme (GLDH) were not retained behind the film. This suggests that the film may actually be porous and that in solution the pores increase in size with egress of the biocomponents.

Layer 3 shows a more compact structure and the underlying biosensor components are less visible than in layer 2. The biosensor comprising all 3 layers produced steady state responses to the addition of glutamate, indicating successful immbolisation of all the components.

3.2. Hydrodynamic Voltammetry

Hydrodynamic voltammetry was performed using the reagentless biosensor with 400 μM of glutamate in 0.75mM phosphate buffer (pH 7.0) containing 50mM NaCl. The optimum potential was considered to be +0.1V vs. Ag/AgCl (Fig 3) as this potential was situated on the plateau of the voltammetric wave.

3.3. Optimisation Studies

Table 2: Performance characteristics of the glutamate biosensor fabricated with different masses of NAD^+ and CHIT using a fixed quantity of GLDH.

GLDH (Units)	NAD^+ (μg)	CHIT (μg)	Linear Range (μM)	Sensitivity (nA/μM)
27	13.5	5	25 – 50	0.035
27	27	5	25 – 100	0.230
27	54	5	25 – 75	0.238
27	106	5	25 – 100	0.307
27	214	5	25 – 50	0.238
27	106	5	25 – 100	0.305
27	106	10	7.5 – 105	0.315
27	106	15	25 – 50	0.261
27	106	20	Steady states not achieved.	N/A

Table 2 shows that the best performance for the glutamate biosensor was achieved with 106 μg NAD^+ and 10 μg of CHIT, together with 27U of GLDH in layer 2, in the absence of MB.

It has been noted by [25], that with increasing concentrations of CHIT, the particle size of untreated MWCNT's in aqueous solution is increased; consequently the larger particle size leads to increasingly entangled molecules of CNT/CHIT resulting in higher visocities. This change in visoscity would lead to a smaller diffusion coefficient, therefore leading to a decrease in the signal. This might explain why loadings of 15 and 20μg resulted in less sensitivity than 10μg in the present study. This also suggests that 5μg may not have

sufficiently bound the biological components, in comparison to 10µg of CHIT. Consequently, a CHIT loading of 10µg was selected for further studies.

In order to asses the possibility of enchancing the effectiveness of the electron shuttling through the MWCNTs to the underlying MB electrode, the effect of adding additional MB into these layers was investigated. It was found that the sensitivity was increased from 0.315 nA/µM to 0.396 nA/µM and the linear range was unaltered. Consequently MB was incorporated into all layers of the biosensor for all further studies.

3.4. Linear Range, Sensitivity, Detection Limit and Lifetime of Biosensor

Figure 5A shows a typical amperogram obtained with the optimised biosensor for different concentrations of glutamate. The inset (Fig 5B) shows the resulting calibration plots which are linear over the range 7.5 – 105µM, the first calibration plot depicts Fig 5A; the detection limit was 3µM (based on n = 5, the coefficient of variation (CV) was 8.5%), based on three times the signal to noise, and the sensitivity was 0.39 nA/µM (based on n =5, the CV was 6.37%). It should be noted that the biosensor possesses sensitivity relative to surface area of 4.3µA/mM/cm^2. This behaviour demonstrates the possibility of applying this device to food and biological samples.

The life time of the biosensor in continuous operation is 2 hours, whilst the shelf lifetime is at least 2 weeks without any change in sensitivity. For the latter study, biosensors were stored in a desiccator which was stored in a fridge at 4°C. It should be mentioned that biosensors based on the cofactor NAD^+ can be readily stabilised for over six months using commercially available enzyme stabilisers [26]. The life time of the biosensor was determined by calibration studies with known additions of glutamate in buffer (pH 7, 35°C). The sensitivity was then determined based on the slope of the subsequent calibration plots (n = 3).

3.5. Optimisation of Temperature and pH

The optimum pH was determined by carrying out calibration studies over the pH range 5 – 9 at a temperature of 25°C. The optimum pH was determined to be pH 7 as biosensors achieved the greatest sensitivity at this pH. A neutral pH also ensures that further studies investigating food and serum will not require the pH to be changed to achieve maximum sensitivity, thereby reducing sample preparation steps. A separate study was conducted to determine the optimum temperature. The temperature was varied over the range 25 – 40°C with the pH fixed at 7. The optimum temperature was determined to be 35°C.

3.6. Application of the optimum amperometric biosensor (MWCNT–CHIT–MB/GLDH–NAD–CHIT–MB/MWCNT–CHIT–MB) to the determination of glutamate in unspiked food.

Many food products are known to contain MSG as a flavour enhancer, therefore, we decided to apply our new reagentless biosensor to determine glutamate in a known brand of beef stock cube.

Standard addition was conducted by dissolving one OXO cube (5.9 g mass) in 50ml of PB and sonicating for 15 minutes until fully dissolved. Five replicate aliquots from this solution were analysed using fresh reagentless biosensors for each measurement. The determination was performed by adding an aliquot of PBS (9.95 mL) to the voltammetric cell, establishing a steady state current, and then injecting a 5µL volume of the OXO cube/PB solution into the cell. Sequential 3µL injections of 25 mM glutamate were then added to the cell, standard addition plots were constructed and from these the endogenous glutamate concentration was determined (n = 5). The mean quantity of glutamate recovered in unspiked OXO Cubes was 90.6 mg/g, with a CV of 7.52%; results are shown in Table 3. A typical amperogram obtained

from the analysis of an OXO cube utilising the reagentless biosensor is shown in Figure 3 in the supplementary material.

The average percentage of glutamate was calculated relative to the mass of an OXO cube and was found to be 18.1% (± 1.36%, n = 5). This compares favourably with a previously published value for MSG content in OXO cubes [7]. The quantity of glutamate recovered from the stock cube compares favourably with levels calculated with an optical biosensor, validated with HPLC [27] and utilising high performance thin layer chromatography [28]. The optical biosensor and HPLC analysis determined an L-glutamate level of 18.29% (± 0.66%) and 17.70% (± 0.34%) based on n = 3, whilst the high performance thin layer chromatography technique determined a level of 133.50 mg/g (± 0.84%, n = 3). These values compare favourably to the values we have determined utilising the reagentless biosensor.

Table 3: Quantity of glutamate determined in an unspiked beef OXO cube and in unspiked foetal bovine serum.

OXO Cube Sample	Quantity of Glutamate Recovered (mg/g)	Unspiked Foetal Bovine Serum Sample	Concentration of Glutamate Detected (mM)
1	92.33	1	1.45
2	91.48	2	1.60
3	96.73	3	1.33
4	94.83	4	1.30
5	77.47	5	1.51

Mean (mg/g)	90.56	Mean (mM)	1.44
Std Dev	6.81	Std Dev	0.12
CV (%)	7.52	Cov (%)	8.54

3.7. Application of the optimum amperometric biosensor (MWCNT–CHIT–MB/GLDH–NAD–CHIT–MB/MWCNT–CHIT–MB) to the determination of glutamate in both unspiked and spiked serum.

Amperometry, in conjunction with standard addition, was used to determine the endogenous levels of glutamate and the recovery for serum spiked with additional glutamate. The replicate serum samples were analysed using a fresh biosensor for each measurement. A typical amperogram obtained from the analysis of unspiked serum utilising the reagentless biosensor is shown in Figure 4 in the supplementary material.

The data obtained on serum samples using the glutamate biosensor are shown in Table 3. The mean endogenous level of glutamate detected was 1.44 mM for the unspiked samples. The coefficient of variation was 8.54% for the five individual samples. This value is comparable to our previous publication [7] in which we report a value of 1.68 mM. It is worth noting this also compares favourably to a value discovered by a bioluminescence method [29].

The biosensors were then used to determine glutamate in spiked serum by fortifying with 1.50 mM of glutamate. The results are shown in Table 4. The mean recovery (n = 5) was 104% with a CV of 2.91%.

Table 4: Recovery of glutamate detected in spiked serum fortified with additional glutamate.

Sample	Fortified Glutamate (mM)	Endogenous Concentration (mM)	Concentration of Glutamate Detected (mM)	Recovery (%)
1	1.50	1.44	2.96	101

2	1.50	1.44	3.01	105
3	1.50	1.44	3.02	105
4	1.50	1.44	2.97	102
5	1.50	1.44	3.07	109

Mean recovery (%)	104
Std Dev	3
Cov (%)	2.91

4. Conclusion

This paper has described the successful development of a reagentless amperometric glutamate biosensor. This was achieved by incorporating the biocomponents using a layer-by-layer procedure involving chitosan and MWCNTs. The device produced well defined steady state currents over extended operating times indicating that the bio-components are securely immobilised onto the base transducer.

The reagentless glutamate biosensor, fabricated in this study, is to date the first of its kind; our biosensor detection limit compares favourably to those previously reported for non-reagentless glutamate sensors. The limit of detection of our biosensor is 3 µM, whereas detection limits of 3.8µM, 10µM, 300µM, 5µM, 5µM, 20µM, 28µM and 50µM were reported by Alvarez-Crespo et al., 1997; Mizutani et al., 1998; Pasco et al., 1999; Schuvailo et al., 2007; Tsukatani and Matsumoto, 2005; Ye et al., 1995, Monošík et al., 2013, Doaga et al., 2009, respectively.

The device and its components have been fully optimised to produce a reproducible reagentless biosensor which has been applied to the analysis of glutamate in clinical and food samples. Notably, the samples required no pre-treatment, other than dilution. The content of glutamate determined in OXO cubes and in serum compares favourably to that determined with our previous glutamate biosensor [7].

This novel layer-by-layer approach to biosensor fabrication may hold promise as a generic platform for future biosensors based on dehydrogenase systems.

It should be mentioned that the analysis of neuronal cells for changes in glutamate flux is of significant biomedical interest. High levels of glutamate leads to excitotoxicity, which is associated with diseases previously mentioned in the introduction. For potential future studies and applications, it is of value to consider how our biosensor compares to previously reported sensors which determine neuronal glutamate.

Previously reported microelectrodes have been used to measure glutamate *in vivo* in rodent studies; these were fabricated by coating microelectrodes with glutamate oxidase (Burmeister and Gerhardt, 2003; Frey et al., 2010; Hu et al., 1994; McLamore et al., 2010; Qin et al., 2008; Tian et al., 2009; Wassum et al., 2008). These required high operating potentials (+600 - 700mV vs. Ag/AgCl), as the detection system involved the measurement of hydrogen

peroxide. High operating potentials can lead to the oxidisation of interferences such as ascorbic acid, which can interfere the measurement of glutamate. It is worth noting that Oldenziel et al., 2006, utilised a lower operating potential of +150mV vs. Ag/AgCl, by utilising the electron mediator horseradish peroxidase; which increased the complexity of biosensor fabrication.

Microelectrodes coated with glutamate dehydrogenase are uncommon; this is likely due to the requirement of integrating the cofactor NAD^+ onto the surface of the microelectrode without leeching, as mentioned previously. By miniaturizing our reagentless biosensor, the lower operating potential required to generate an analytical response would prove beneficial for the analysis of glutamate in real time, in neuronal cells. Our approach would negate the requirement for additional enzymes or use of charged membranes such as Nafion, to block out potential interferences. It should be feasible to incorporate the approach described in this paper into a implantable system by dip coating a carbon fibre electrode (10µM diameter) into formulation described in this paper.

Acknowledgements

The authors wish to thank the University of the West of England, Bristol for funding. Gwent Electronic Materials are thanked for the provision of the MB–SPCEs. Thanks to Dr D. Patton for his help in obtaining the SEM images.

References

[1] A. Ghanizadeh, "Increased glutamate and homocysteine and decreased glutamine levels in autism: a review and strategies for future studies of amino acids in autism.," *Dis. Markers*, vol. 35, no. 5, pp. 281–6, Jan. 2013.

[2] A. Davalos, J. Castillo, J. Serena, and M. Noya, "Duration of Glutamate Release After Acute Ischemic Stroke," *Stroke*, vol. 28, no. 4, pp. 708–710, Apr. 1997.

[3] J. T. Greenamyre, W. F. Maragos, R. L. Albin, J. B. Penney, and A. B. Young, "Glutamate transmission and toxicity in Alzheimer's disease.," *Prog. Neuropsychopharmacol. Biol. Psychiatry*, vol. 12, no. 4, pp. 421–30, Jan. 1988.

[4] D. C. Javitt, "Glutamatergic theories of schizophrenia.," *Isr. J. Psychiatry Relat. Sci.*, vol. 47, no. 1, pp. 4–16, Jan. 2010.

[5] I. A. Paul and P. Skolnick, "Glutamate and depression: clinical and preclinical studies.," *Ann. N. Y. Acad. Sci.*, vol. 1003, pp. 250–72, Nov. 2003.

[6] R. Monosik, M. Stredansky, J. Tkac, and E. Sturdik, "Application of Enzyme Biosensors in Analysis of Food and Beverages," *Food Anal. Methods*, vol. 5, no. 1, pp. 40–53, Mar. 2011.

[7] G. Hughes, R. M. Pemberton, P. R. Fielden, and J. P. Hart, "Development of a Disposable Screen Printed Amperometric Biosensor Based on Glutamate Dehydrogenase, for the Determination of Glutamate in Clinical and Food Applications," *Anal. Bioanal. Electrochem.*, vol. 6, no. 4, pp. 435–449, 2014.

[8] J. Wang, "Carbon-Nanotube Based Electrochemical Biosensors: A Review," *Electroanalysis*, vol. 17, no. 1, pp. 7–14, Jan. 2005.

[9] M. Zhang, A. Smith, and W. Gorski, "Carbon nanotube-chitosan system for electrochemical sensing based on dehydrogenase enzymes.," *Anal. Chem.*, vol. 76, no. 17, pp. 5045–50, Sep. 2004.

[10] J. M. Nugent, K. S. V. Santhanam, A. Rubio, and P. M. Ajayan, "Fast Electron Transfer Kinetics on Multiwalled Carbon Nanotube Microbundle Electrodes," *Nano Lett.*, vol. 1, no. 2, pp. 87–91, Feb. 2001.

[11] L. Zhu, J. Zhai, R. Yang, C. Tian, and L. Guo, "Electrocatalytic oxidation of NADH with Meldola's blue functionalized carbon nanotubes electrodes," 2007.

[12] M. Boujtita, J. P. Hart, and R. Pittson, "Development of a disposable ethanol biosensor based on a chemically modified screen-printed electrode coated with alcohol oxidase for the analysis of beer.," *Biosens. Bioelectron.*, vol. 15, no. 5–6, pp. 257–63, Aug. 2000.

[13] A. C. Pereira, M. R. Aguiar, A. Kisner, D. V. Macedo, and L. T. Kubota, "Amperometric biosensor for lactate based on lactate dehydrogenase and Meldola Blue coimmobilized on multi-wall carbon-nanotube," *Sensors Actuators B Chem.*, vol. 124, no. 1, pp. 269–276, Jun. 2007.

[14] S. D. Sprules, J. P. Hart, S. A. Wring, and R. Pittson, "Development of a disposable amperometric sensor for reduced nicotinamide adenine dinucleotide based on a chemically modified screen-printed carbon electrode," *Analyst*, vol. 119, no. 2, p. 253, Jan. 1994.

[15] L. Qian and X. Yang, “Composite film of carbon nanotubes and chitosan for preparation of amperometric hydrogen peroxide biosensor.,” *Talanta*, vol. 68, no. 3, pp. 721–7, Jan. 2006.

[16] H. J. Malmiri, M. Ali, G. Jahanian, and A. Berenjian, “Potential Applications of Chitosan Nanoparticles As Novel Support in Enzyme Immobilization,” *Am. J. Biochem. Biotechnol.*, vol. 8, no. 4, pp. 203–219, Apr. 2012.

[17] O. V. Kharissova, B. I. Kharisov, and E. G. de Casas Ortiz, “Dispersion of carbon nanotubes in water and non-aqueous solvents,” *RSC Adv.*, vol. 3, no. 47, p. 24812, Nov. 2013.

[18] M. Zhang, C. Mullens, and W. Gorski, “Coimmobilization of Dehydrogenases and Their Cofactors in Electrochemical Biosensors,” *Anal. Chem.*, vol. 79, no. 6, pp. 2446–2450, Mar. 2007.

[19] B.-Y. Wu, S.-H. Hou, F. Yin, J. Li, Z.-X. Zhao, J.-D. Huang, and Q. Chen, “Amperometric glucose biosensor based on layer-by-layer assembly of multilayer films composed of chitosan, gold nanoparticles and glucose oxidase modified Pt electrode.,” *Biosens. Bioelectron.*, vol. 22, no. 6, pp. 838–44, Jan. 2007.

[20] H. Zhao and H. Ju, “Multilayer membranes for glucose biosensing via layer-by-layer assembly of multiwall carbon nanotubes and glucose oxidase.,” *Anal. Biochem.*, vol. 350, no. 1, pp. 138–44, Mar. 2006.

[21] X. Zhou, F. Xi, Y. Zhang, and X. Lin, “Reagentless biosensor based on layer-by-layer assembly of functional multiwall carbon nanotubes and enzyme-mediator biocomposite,” *J. Zhejiang Univ. Sci. B*, vol. 12, no. 6, pp. 468–476, Jun. 2011.

[22] K. Ariga, J. P. Hill, and Q. Ji, “Layer-by-layer assembly as a versatile bottom-up nanofabrication technique for exploratory research and realistic application.,” *Phys. Chem. Chem. Phys.*, vol. 9, no. 19, pp. 2319–40, May 2007.

[23] E. J. Cho, J.-W. Lee, M. Rajdendran, and A. D. Ellington, *Optical Biosensors: Today and Tomorrow*. Elsevier, 2011.

[24] R. C. Alkire, D. M. Kolb, and J. Lipkowski, Eds., *Advances in Electrochemical Science and Engineering*. Weinheim, Germany: Wiley-VCH Verlag GmbH & Co. KGaA, 2011.

[25] Y.-T. Shieh, H.-M. Wu, Y.-K. Twu, and Y.-C. Chung, “An investigation on dispersion of carbon nanotubes in chitosan aqueous solutions,” *Colloid Polym. Sci.*, vol. 288, no. 4, pp. 377–385, Oct. 2009.

[26] M. Piano, S. Serban, N. Biddle, R. Pittson, G. A. Drago, and J. P. Hart, “A flow injection system, comprising a biosensor based on a screen-printed carbon electrode containing Meldola’s Blue-Reinecke salt coated with glucose dehydrogenase, for the measurement of glucose.,” *Anal. Biochem.*, vol. 396, no. 2, pp. 269–74, Jan. 2010.

[27] N. Z. Md Muslim, M. Ahmad, L. Y. Heng, and B. Saad, “Optical biosensor test strip for the screening and direct determination of l-glutamate in food samples,” *Sensors Actuators B Chem.*, vol. 161, no. 1, pp. 493–497, Jan. 2012.

[28] V. N. Krishna, D. Karthika, D. M. Surya, M. Rubini, M. Vishalini, and Y. Pradeepa, “Analysis of Monosodium l-Glutamate in Food Products by High-Performance Thin Layer Chromatography.,” *J. Young Pharm.*, vol. 2, no. 3, pp. 297–300, Jul. 2010.

[29] Z. C. Ye and H. Sontheimer, “Astrocytes protect neurons from neurotoxic injury by serum glutamate.,” *Glia*, vol. 22, no. 3, pp. 237–48, Mar. 1998.

[30] F. Mizutani, Y. Sato, Y. Hirata, and S. Yabuki, “High-throughput flow-injection analysis of glucose and glutamate in food and biological samples by using enzyme/polyion complex-bilayer membrane-based electrodes as the detectors,” *Biosens. Bioelectron.*, vol. 13, no. 7–8, pp. 809–815, Oct. 1998.

[31] N. Pasco, C. Jeffries, Q. Davies, A. J. Downard, A. D. Roddick-Lanzilotta, and L. Gorton, “Characterisation of a thermophilic L-glutamate dehydrogenase biosensor for amperometric determination of L-glutamate by flow injection analysis,” *Biosens. Bioelectron.*, vol. 14, no. 2, pp. 171–178, Feb. 1999.

[32] R. J. Cosford and W. G. Kuhr, “Capillary biosensor for glutamate.,” *Anal. Chem.*, vol. 68, no. 13, pp. 2164–2169, 1996.

[33] W. Laiwattanapaisal and J. Yakovleva, “On-chip microfluidic systems for determination of L-glutamate based on enzymatic recycling of substrate,” *Biomicrofluidics*, vol. 3, no. 1, p. 14104, Jan. 2009.

[34] O. M. Schuvailo, S. Gáspár, A. P. Soldatkin, and E. Csöregi, “Ultramicrobiosensor for the Selective Detection of Glutamate,” *Electroanalysis*, vol. 19, no. 1, pp. 71–78, Jan. 2007.

[35] B.-C. Ye, Q.-S. Li, Y.-R. Li, X.-B. Li, and J.-T. Yu, “l-Glutamate biosensor using a novel l-glutamate oxidase and its application to flow injection analysis system,” *J. Biotechnol.*, vol. 42, no. 1, pp. 45–52, Aug. 1995.

[36] T. Tsukatani and K. Matsumoto, “Sequential fluorometric quantification of γ-aminobutyrate and l-glutamate using a single line flow-injection system with immobilized-enzyme reactors,” *Anal. Chim. Acta*, vol. 546, no. 2, pp. 154–160, Aug. 2005.

[37] S. L. Alvarez-Crespo, M. J. Lobo-Castañón, A. J. Miranda-Ordieres, and P. Tuñón-Blanco, “Amperometric glutamate biosensor based on poly(o-phenylenediamine) film electrogenerated onto modified carbon paste electrodes,” *Biosens. Bioelectron.*, vol. 12, no. 8, pp. 739–747, Jul. 1997.

[38] R. Monošík, M. Streďanský, and E. Šturdík, “A Biosensor Utilizing l-Glutamate Dehydrogenase and Diaphorase Immobilized on Nanocomposite Electrode for Determination of l-Glutamate in Food Samples,” *Food Anal. Methods*, vol. 6, no. 2, pp. 521–527, Jul. 2013.

[39] R. Doaga, T. McCormac, and E. Dempsey, “Electrochemical Sensing of NADH and Glutamate Based on Meldola Blue in 1,2-Diaminobenzene and 3,4-Ethylenedioxythiophene Polymer Films,” *Electroanalysis*, vol. 21, no. 19, pp. 2099–2108, Oct. 2009.

[40] J. J. Burmeister and G. A. Gerhardt, “Ceramic-based multisite microelectrode arrays for in vivo electrochemical recordings of glutamate and other neurochemicals,” *TrAC Trends Anal. Chem.*, vol. 22, no. 8, pp. 498–502, Sep. 2003.

[41] O. Frey, T. Holtzman, R. M. McNamara, D. E. H. Theobald, P. D. van der Wal, N. F. de Rooij, J. W. Dalley, and M. Koudelka-Hep, “Enzyme-based choline and L-glutamate biosensor electrodes on silicon microprobe arrays.,” *Biosens. Bioelectron.*, vol. 26, no. 2, pp. 477–84, Oct. 2010.

[42] E. S. McLamore, S. Mohanty, J. Shi, J. Claussen, S. S. Jedlicka, J. L. Rickus, and D. M. Porterfield, “A self-referencing glutamate biosensor for measuring real time neuronal glutamate flux.,” *J. Neurosci. Methods*, vol. 189, no. 1, pp. 14–22, May 2010.

[43] W. H. Oldenziel, G. Dijkstra, T. I. F. H. Cremers, and B. H. C. Westerink, “In vivo monitoring of extracellular glutamate in the brain with a microsensor.,” *Brain Res.*, vol. 1118, no. 1, pp. 34–42, Nov. 2006.

[44] S. Qin, M. van der Zeyden, W. H. Oldenziel, T. I. F. H. Cremers, and B. H. C. Westerink, “Microsensors for in vivo Measurement of Glutamate in Brain Tissue,” *Sensors*, vol. 8, no. 11, pp. 6860–6884, Nov. 2008.

[45] K. M. Wassum, V. M. Tolosa, J. Wang, E. Walker, H. G. Monbouquette, and N. T. Maidment, “Silicon Wafer-Based Platinum Microelectrode Array Biosensor for Near Real-Time Measurement of Glutamate in Vivo,” *Sensors*, vol. 8, no. 8, pp. 5023–5036, Aug. 2008.

[46] Y. Hu, K. M. Mitchell, F. N. Albahadily, E. K. Michaelis, and G. S. Wilson, “Direct measurement of glutamate release in the brain using a dual enzyme-based electrochemical sensor,” *Brain Res.*, vol. 659, no. 1–2, pp. 117–125, Oct. 1994.

[47] F. Tian, A. V Gourine, R. T. R. Huckstepp, and N. Dale, “A microelectrode biosensor for real time monitoring of L-glutamate release.,” *Anal. Chim. Acta*, vol. 645, no. 1–2, pp. 86–91, Jul. 2009.

Figure and Scheme Captions

Fig 1. A schematic diagram displaying the layer-by-layer drop coating fabrication procedure used to construct the reagentless glutamate biosensor, based on a MB-SPCE electrode.

Fig 2. Schematic displaying the interaction between the immobilized enzyme GLDH and glutamate at the surface of the electrode and the subsequent generation of the analytical response.

Fig 3. Hydrodynamic voltammograms obtained using MB-SPCE/MWCNT-CHIT-MB/GLDH-NAD^+-CHIT-MB/MWCNT-CHIT-MB biosensor in the presence of 400μM glutamate in 75mM phosphate buffer (pH 7.0) containing 50 mM NaCl.

Fig 4. SEM imaging of each individual layer of the reagentless biosensor. The scale is the same for all SEM images.

Fig 5. **A)** Amperogram conducted with the proposed final biosensor. Each arrow represents an injection of 3μL of 25mM glutamate in a 10mL stirred solution containing supporting electrolyte; 75mM, PB (pH 7.0), with 50mM NaCl at an applied potential of +0.1V vs. Ag/AgCl.

B) Calibration plots of five individually tested biosensors. The amperogram is depicted in the first calibration plot.

Supplementary Figures

Fig 1. Temperature study conducted over the range of 25 to 40°C. Values represent average currents generated at 30μM (n = 3).

Fig 2. pH study conducted over the range of pH 5 to 9. Values represent average currents generated at 15μM (n = 3).

Fig 3. Amperogram displaying the response obtained for unspiked OXO cube followed by two additions of 7.5μM glutamate. 75mM, PB (pH 7.0), with 50mM NaCl at an applied potential of +0.1V vs. Ag/AgCl.

Fig 4. Amperogram displaying the response obtained for unspiked serum followed by two additions of 7.5μM glutamate. 75mM, PB (pH 7.0), with 50mM NaCl at an applied potential of +0.1V vs. Ag/AgCl.

Fig 5. Photograph with scale of the final biosensors with insulating tape attached.

Highlights

- First report on the fabrication of a reagentless amperometric glutamate biosensor using MWCNT's.
- High reproducibility, low cost due to screen printing and ease of use for real samples.
- Detection limit of 3 μM, linear range; 7.5–105 μM and a sensitivity; 0.39 nA/μM.

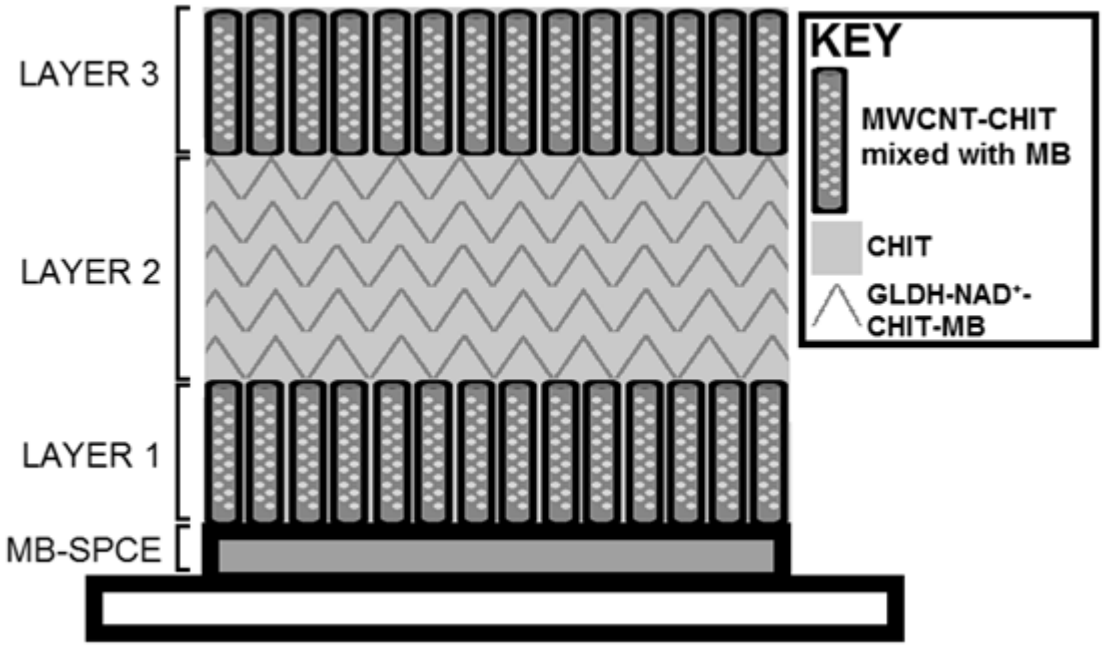

Figure 1 - BW

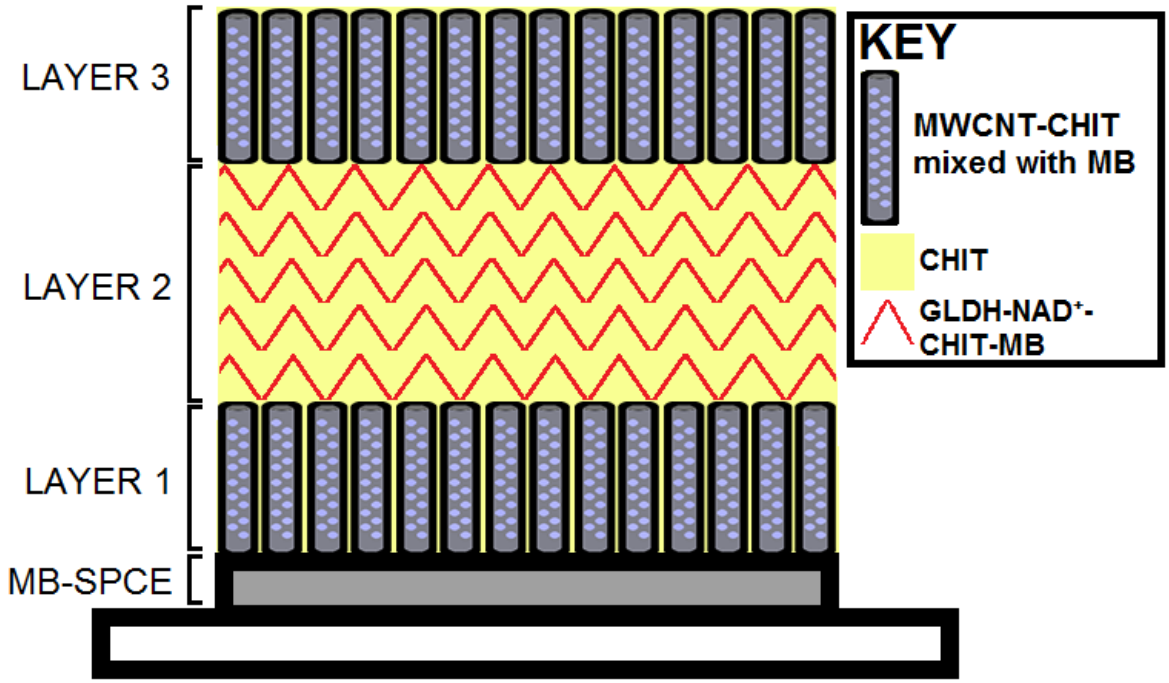

Figure 1 – Colour

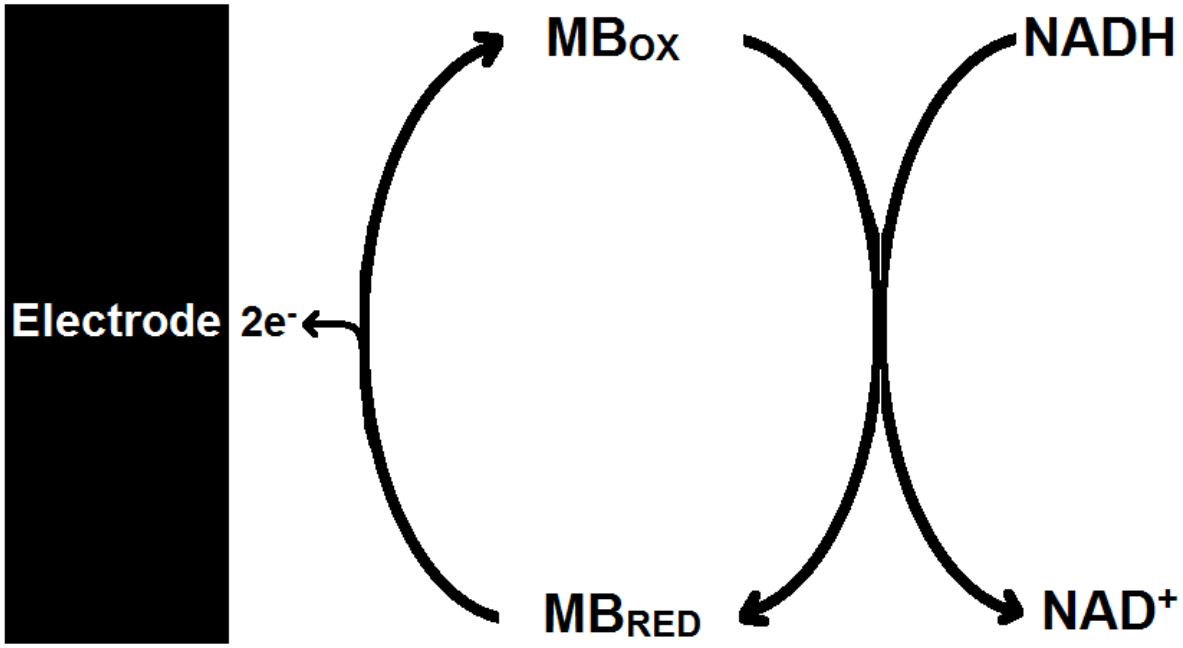

Figure 2

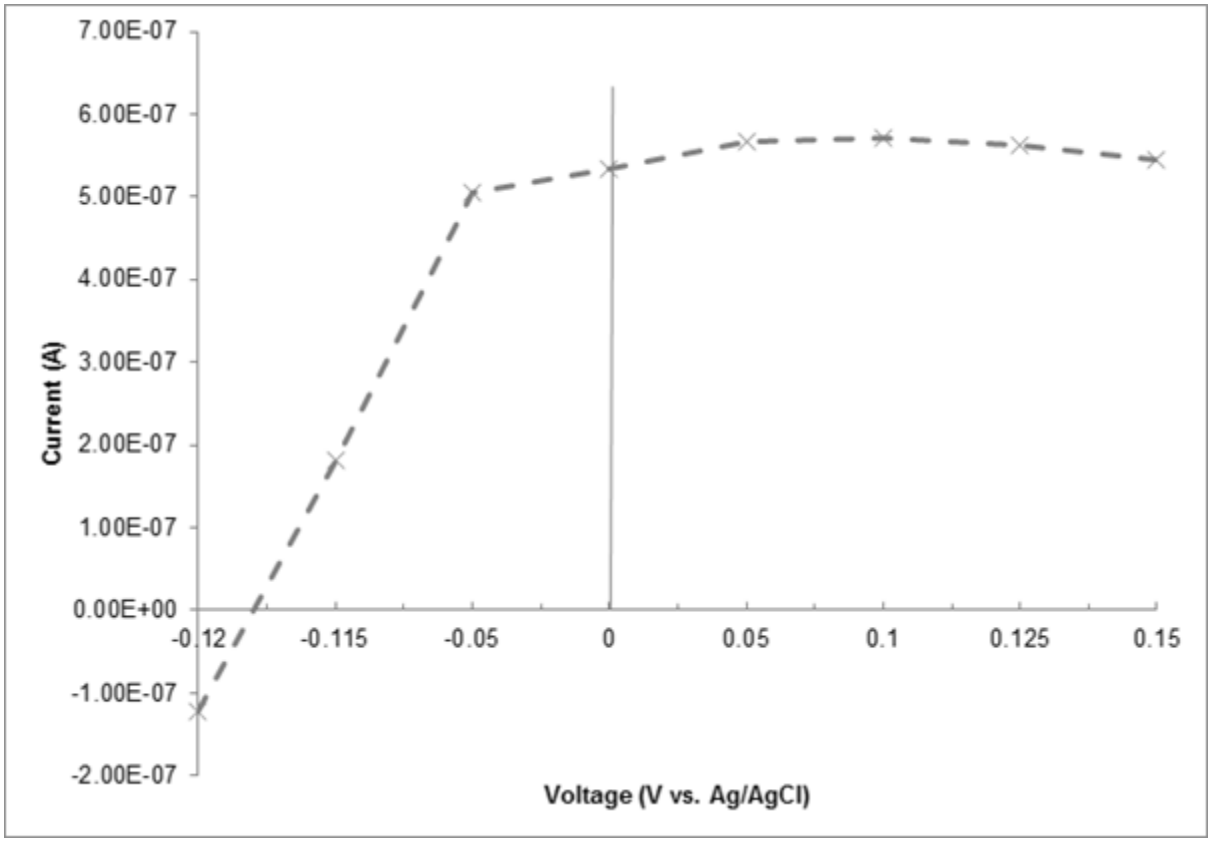

Figure Three – BW

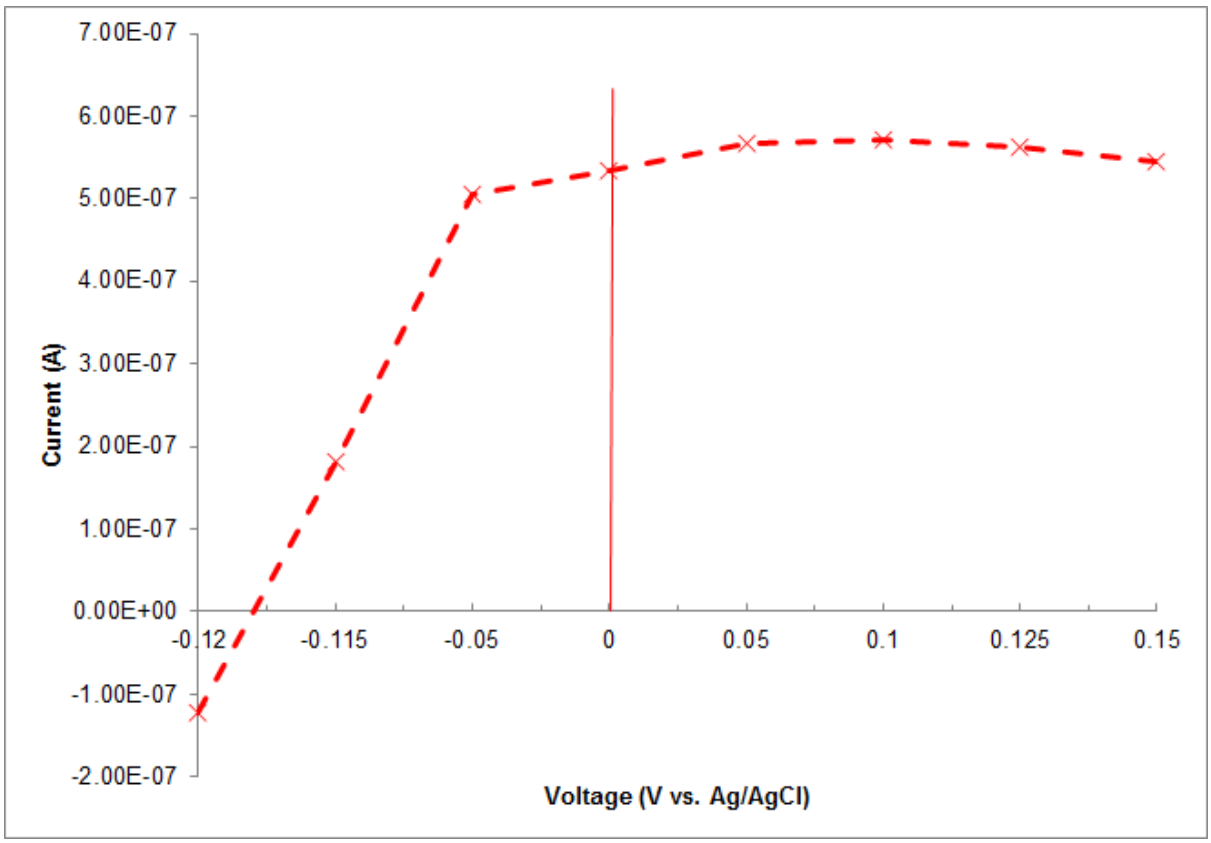

Figure Three – Colour

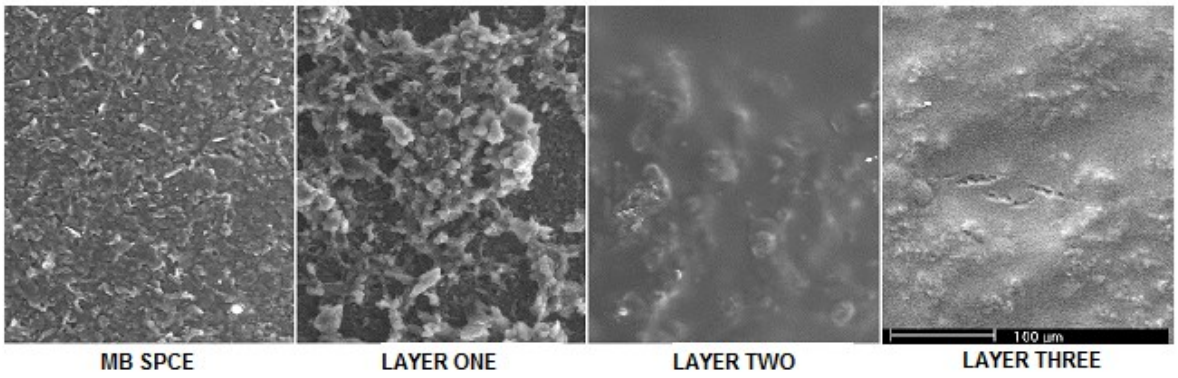

Figure 4

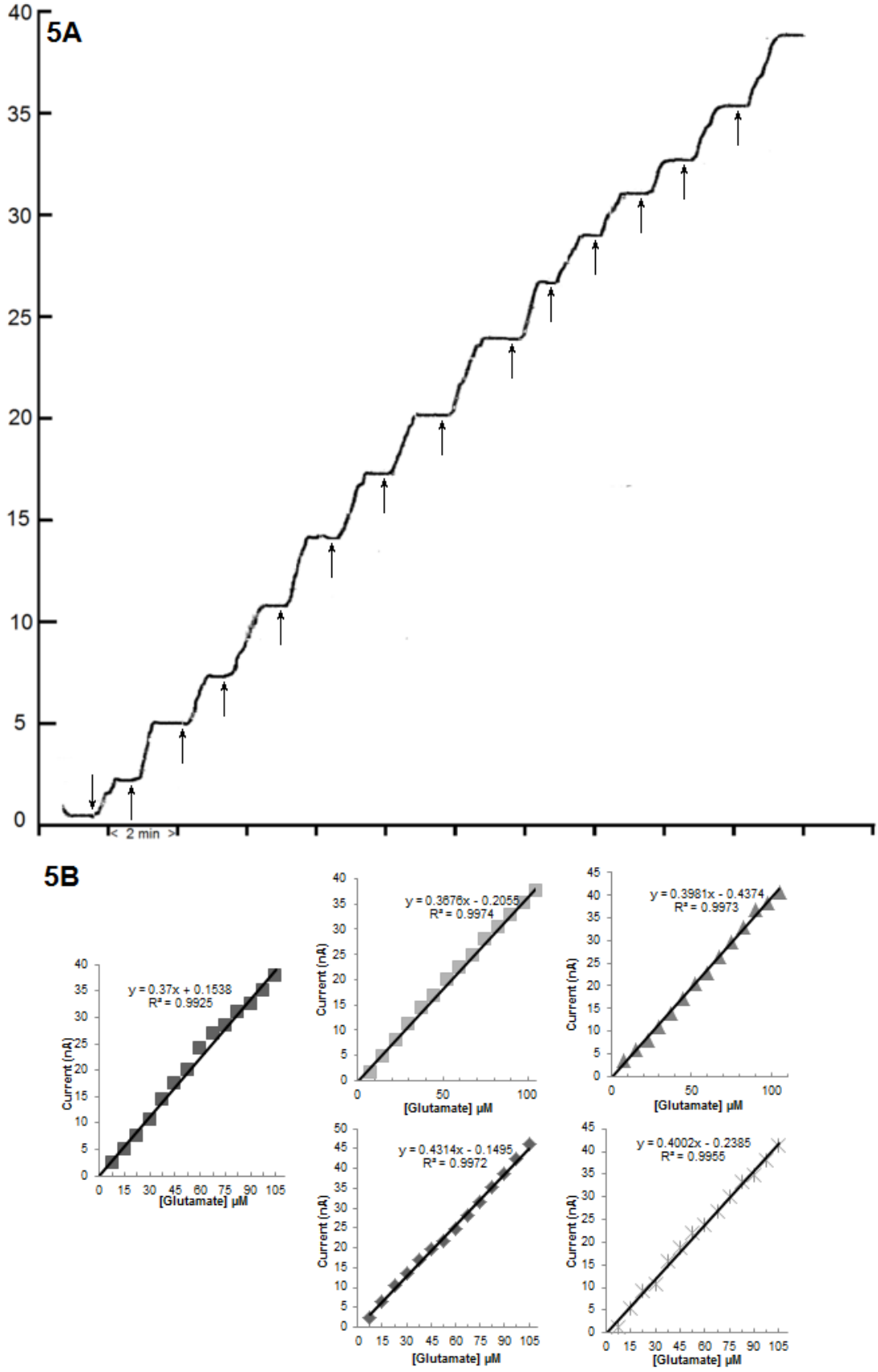
5A
40
35
30
25
20
15
10
5
0
< 2 min >
5B
y = 0.37x + 0.1538
R² = 0.9925
y = 0.3676x - 0.2055
R² = 0.9974
y = 0.3981x - 0.4374
R² = 0.9973
y = 0.4314x - 0.1495
R² = 0.9972
y = 0.4002x - 0.2385
R² = 0.9955
Current (nA)
[Glutamate] µM

Figure 5

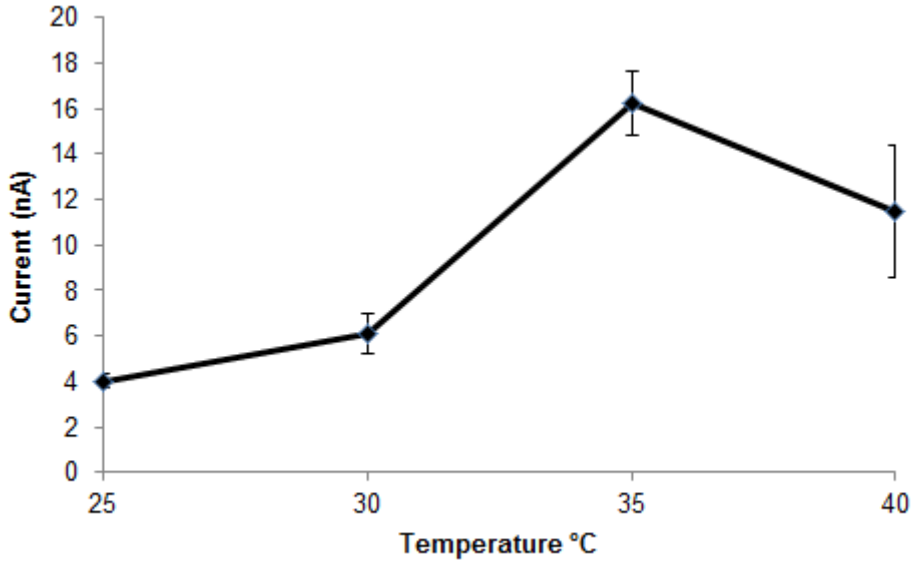

Supp Fig 1

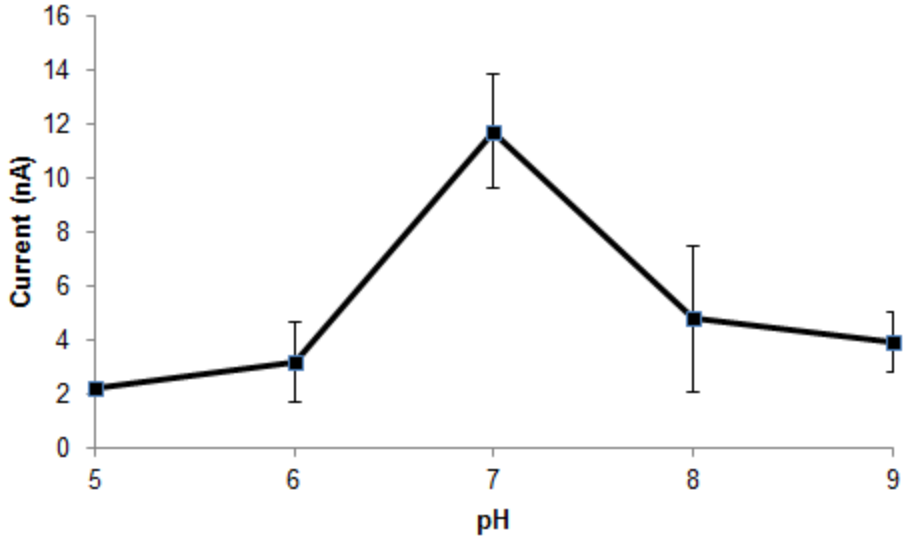

Supp Figure 2

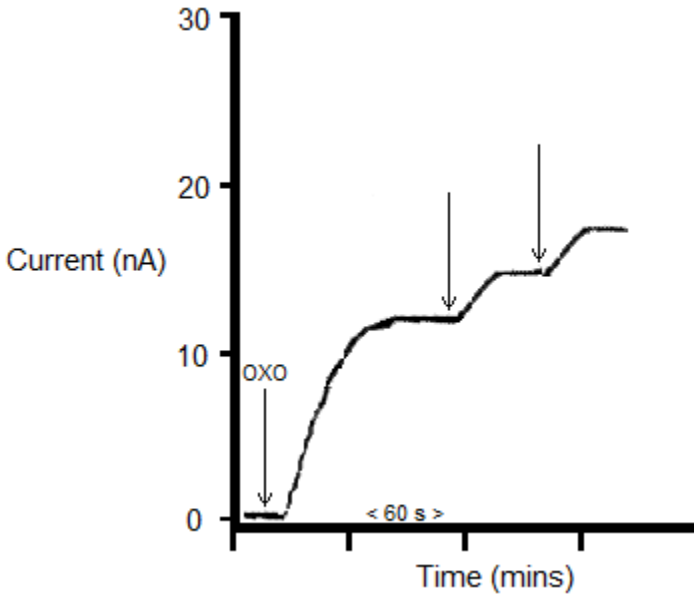

Supp Figure 3

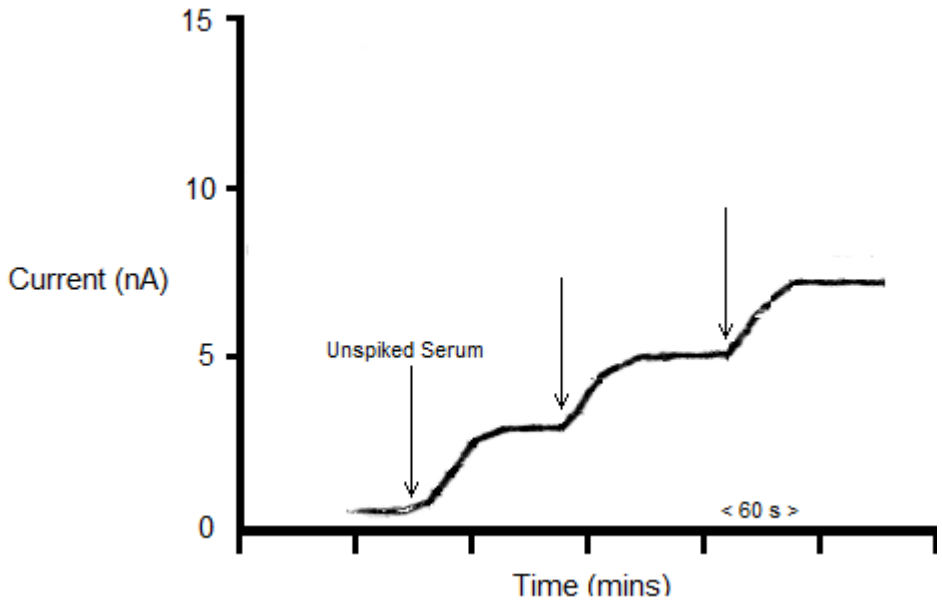

Supp Figure 4

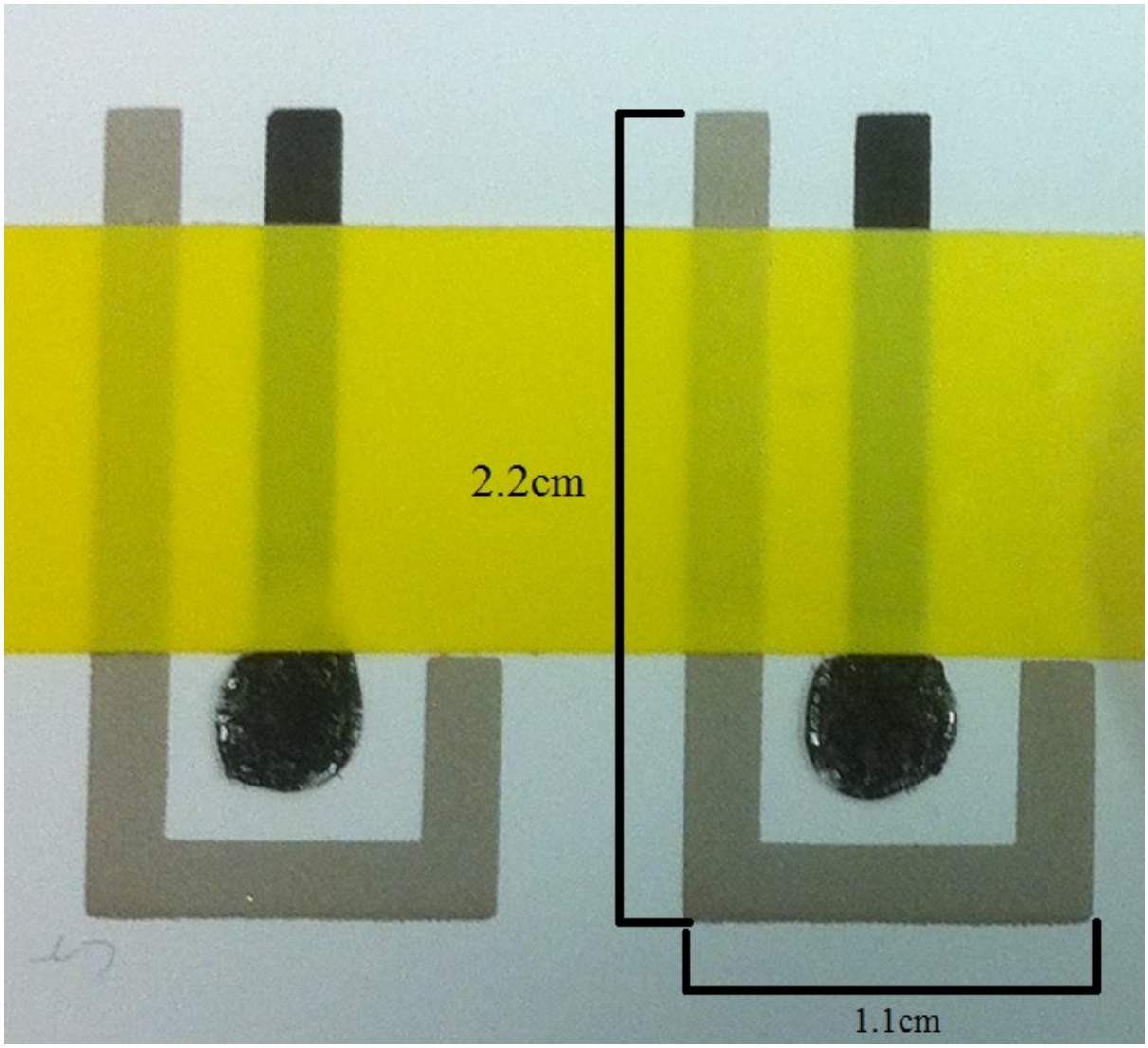

Supp Fig 5.